Hadronic contributions to the muon $g-2$ in a dispersive approach

in collab. with M. Hoferichter and B. Kubis
JHEP **1908** (2019) 137 [arXiv:1907.01556 [hep-ph]]

and with S. Leupold and S. P. Schneider
JHEP **1810** (2018) 141, [arXiv:1808.04823 [hep-ph]]
Phys. Rev. Lett. **121** (2018) 112002, [arXiv:1805.01471 [hep-ph]]

Bai-Long Hoid

Institute for Theoretical Physics
University of Bern

11th May 2021

Outline

Muon anomaly & dispersion relations

Hadronic vacuum polarization

- Overview & dispersive approach
- 3π contribution

Hadronic light-by-light scattering

- Overview & dispersive approach
- Pion-pole contribution

Conclusion and outlook

Muon anomaly & dispersion relations

The muon $g_\mu - 2$:

The magnetic dipole moment of a charged lepton ($\ell = e,\ \mu,\ \tau$):

$$\boldsymbol{\mu}_\ell = g_\ell \left(\frac{Qe}{2m_\ell} \right) \boldsymbol{S}$$

- Dirac equation universally predicts $g_\ell = 2$
- Quantum loop corrections lead to a deviation from the classical Dirac value 2

Define the lepton anomalous magnetic moment (lepton anomaly):

$$a_\ell \equiv \frac{g_\ell - 2}{2}$$

Muon anomaly & dispersion relations

The muon $g_\mu - 2$:

- A pure dimensionless number that can be both theoretically calculated and experimentally measured
- Contributions from a heavy scale M usually: $\propto m_\ell^2/M^2$
- τ is so shortly lived; a_μ is more sensitive than a_e by a factor of $\sim 4 \times 10^4$
- $a_\mu^{\rm SM} = a_\mu^{\rm QED} + a_\mu^{\rm EW} + \underbrace{a_\mu^{\rm Had}}$
  - Hadronic vacuum polarization (HVP)
  - Hadronic light-by-light (HLbL) scattering

Muon anomaly & dispersion relations

QED $\mathcal{O}(\alpha)$:

Schwinger, 1948

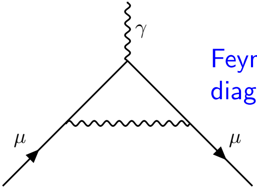

Feynman diagrams

Feynman, 1948

Muon anomaly & dispersion relations

QED $\mathcal{O}(\alpha)$:

Schwinger, 1948

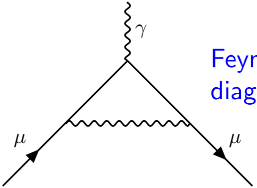

Feynman diagrams

Feynman, 1948

Electroweak one-loop:

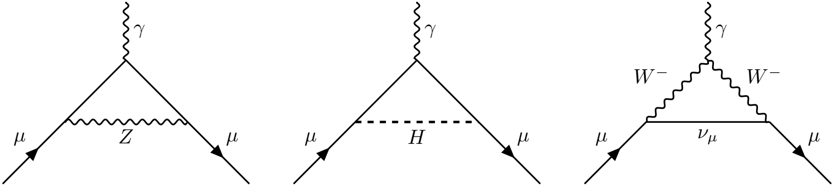

Muon anomaly & dispersion relations

Standard Model contributions to the muon $g_\mu - 2$:

White paper result by the "Muon $g-2$ Theory Initiative" (WP 2020)

Aoyama, ..., B.-L. H. et al., 2020

Contributions	$a_\mu \times 10^{11}$	$\Delta a_\mu \times 10^{11}$
QED (5 loops)	116584718.931	0.104
Electroweak (2 loops)	153.6	1.0
HVP (3 loops)	6845	40
HLbL (3 loops)	92	18
$a_\mu^{\rm SM}$	116591810	43
$a_\mu^{\rm Exp}$	116592061	41
$a_\mu^{\rm Exp} - a_\mu^{\rm SM}$	251	59

Muon anomaly & dispersion relations

$g_\mu - 2$ experiment vs theory:

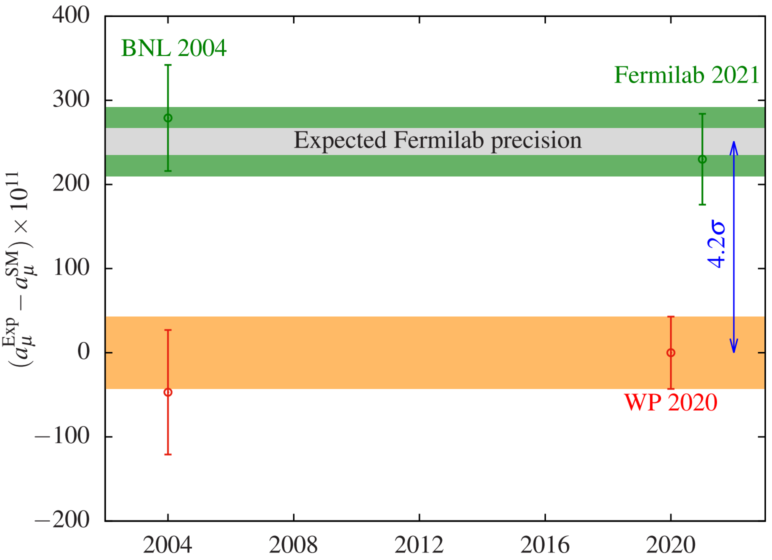

Muon anomaly & dispersion relations

Standard Model theory:

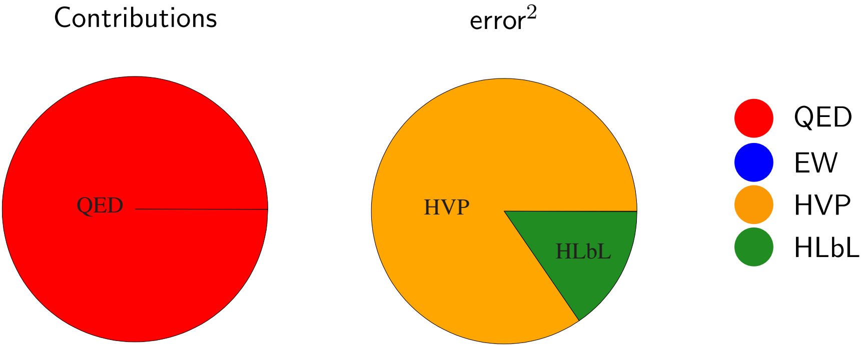

Uncertainties mainly stem form hadronic contributions

Future experiments aim for four-fold improvement $\Delta a_\mu \approx 16 \times 10^{-11}$

$\Rightarrow$ With current theory $\sim 5.5\sigma$

Welcome more precise theoretical predictions

$\Rightarrow$ With theory improvements of same precision $\sim 11\sigma$!

Muon anomaly & dispersion relations

Dispersion relations (DR):

- Microcausality $\Rightarrow$ analyticity
- Unitarity $\Rightarrow 2\,\mathrm{Im}\,M_{fi} = \sum_n \int \mathrm{d}\Pi_n\, M^*_{fn}\, M_{in}$
- Particle-antiparticle transformation $\Rightarrow$ crossing

Combining analyticity, unitarity & crossing:

$$M(s) = \frac{1}{2\pi i}\int_{s_{\rm th}}^{\infty} \frac{\mathrm{disc}\, M(s')}{s'-s}\,\mathrm{d}s' = \frac{1}{\pi}\int_{s_{\rm th}}^{\infty} \frac{\mathrm{Im}\, M(s')}{s'-s}\,\mathrm{d}s'$$

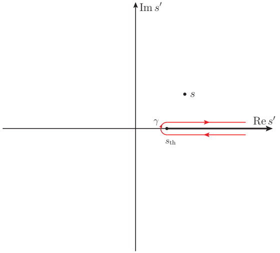

Muon anomaly & dispersion relations

Pion vector form factor $F_\pi^V(s)$:

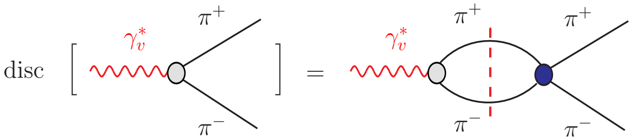

disc $F_\pi^V(s) = 2i\,\mathrm{Im}\,F_\pi^V(s) = 2iF_\pi^V(s)\sin\delta_1^1(s)\,e^{-i\delta_1^1(s)}\theta(s-4M_\pi^2)$

Watson's final-state theorem: phase of $F_\pi^V(s)$ is given by $\delta_1^1(s)$ Watson, 1954

Muon anomaly & dispersion relations

Pion vector form factor $F_\pi^V(s)$:

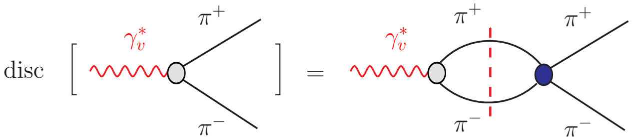

$$\text{disc}\, F_\pi^V(s) = 2i\,\text{Im}\, F_\pi^V(s) = 2iF_\pi^V(s)\sin\delta_1^1(s)\, e^{-i\delta_1^1(s)}\theta(s-4M_\pi^2)$$

Watson's final-state theorem: phase of $F_\pi^V(s)$ is given by $\delta_1^1(s)$ — Watson, 1954

Solution:

$$F_\pi^V(s) = P(s)\Omega(s), \quad \Omega(s) = \exp\left\{\frac{s}{\pi}\int_{4M_\pi^2}^\infty \text{d}s' \frac{\delta_1^1(s')}{s'(s'-s)}\right\}$$

- $\Omega(s)$ is the Omnès function — Omnès, 1958
- $P(s)$ polynomial, $P(0)=1$ from charge conservation
- $\pi\pi$ P-wave phase shift $\delta_1^1(s)$ from Roy equations

Hadronic vacuum polarization

- m_μ as characteristic scale
  $\Rightarrow$ Not a perturbative QCD problem!
- DR to relate to the observable

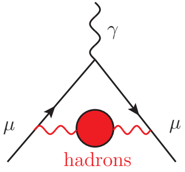

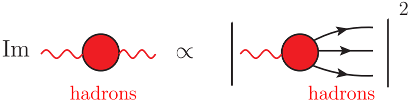

$\propto \quad \sigma(e^+e^- \to \gamma^* \to \text{hadrons})$

$$a_\mu^{\text{HVP}} = \int_{s_{\text{thr}}}^{\infty} \mathrm{d}s K(s) \sigma^0(e^+e^- \to \text{hadrons})$$

- Kinematical function $K(s)$: $K(s) \propto 1/s$ for large s
- $\sigma^0(e^+e^- \to \text{hadrons}) \propto 1/s$ for large s

Hadronic vacuum polarization

Comparison between data-driven approaches and lattice:

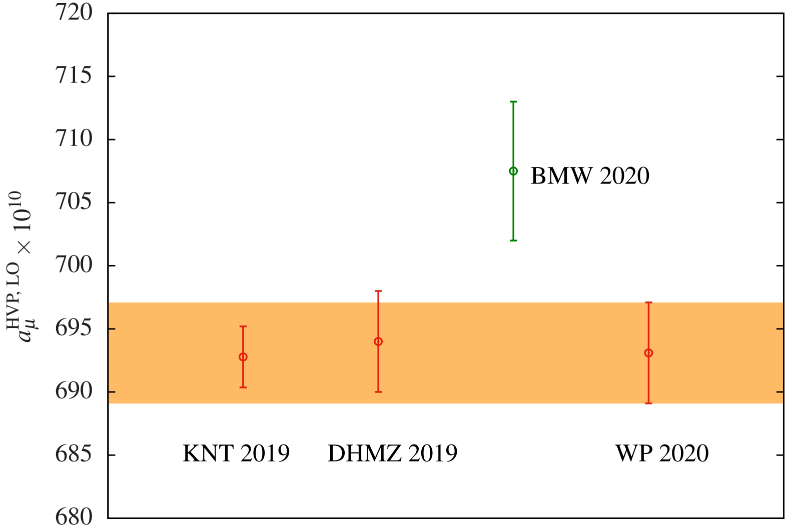

Hadronic vacuum polarization

Complete data-driven evaluation needs:

- Exclusive channels $\pi^+\pi^-$, $\pi^+\pi^-\pi^0$, $\pi^0\gamma$, ...
- Inclusive data
- Perturbative QCD

Hadronic cross section:

- Inclusive of final state radiation
- Exempt from initial state radiation & vacuum polarization (VP)

Overview of the $\pi^+\pi^-\pi^0$ channel

- Second largest exclusive channel after $\pi^+\pi^-$
- Large relative discrepancy between direct data-integration works

$a_\mu^{3\pi} \times 10^{10}$ below $1.8\,\mathrm{GeV}$ before 2019		
Davier et al., 2017	Keshavarzi et al., 2018	relative difference
46.20 ± 1.45	47.70 ± 0.89	3.2% (0.7% for $\pi^+\pi^-$)

Even lower value $a_\mu^{3\pi}|_{\leq 2.0\,\mathrm{GeV}} = 44.3(1.5) \times 10^{-10}$! Jegerlehner, 2017

- Other independent analyses necessary

  $\Rightarrow$ Dispersive global fit function fulfilling analyticity, unitarity & QCD constraints

$\gamma^* \to 3\pi$ dispersive representation

The $\gamma^*(q) \to \pi^+(p_+)\pi^-(p_-)\pi^0(p_0)$ decay amplitude $\mathcal{F}(s,t,u;q^2)$:

$$\langle 0|j_\mu(0)|\pi^+(p_+)\pi^-(p_-)\pi^0(p_0)\rangle = -\epsilon_{\mu\nu\rho\sigma}\, p_+^\nu p_-^\rho p_0^\sigma \mathcal{F}(s,t,u;q^2)$$

$q = p_+ + p_- + p_0$; s, t & u are Mandelstam variables

Decompose into single-variable functions:

$$\mathcal{F}(s,t,u;q^2) = \mathcal{F}(s,q^2) + \mathcal{F}(t,q^2) + \mathcal{F}(u,q^2)$$

Normalization from the Wess–Zumino–Witten (WZW) anomaly:

$$\mathcal{F}(0,0,0;0) = \frac{1}{4\pi^2 F_\pi^3} \equiv F_{3\pi}$$

$F_\pi = 92.28(10)\,\mathrm{MeV}$: pion decay constant P. Zyla et al., 2020

$\gamma^* \to 3\pi$ dispersive representation

Discontinuity equation:

$$\text{disc}\,\mathcal{F}(s,q^2) = 2i(\mathcal{F}(s,q^2) + \hat{\mathcal{F}}(s,q^2))\theta(s-4M_\pi^2)\sin\delta_1^1(s)\,e^{-i\delta_1^1(s)}$$

- $\mathcal{F}(s,q^2)$: right-hand cut
- $\hat{\mathcal{F}}(s,q^2)$: left-hand cut; angular averages of $\mathcal{F}(t,q^2)$ & $\mathcal{F}(u,q^2)$

$\gamma^* \to 3\pi$ dispersive representation

A once-subtracted dispersive solution to the discontinuity equation:

Hoferichter et al., 2014

$$\mathcal{F}(s,q^2) = a(q^2)\Omega(s)\Big\{1 + \frac{s}{\pi}\int_{4M_\pi^2}^{\infty} \mathrm{d}s' \frac{\hat{\mathcal{F}}(s',q^2)\sin\delta_1^1(s')}{s'(s'-s)|\Omega(s')|}\Big\}$$

$$\Omega(s) = \exp\left\{\frac{s}{\pi}\int_{4M_\pi^2}^{\infty} \mathrm{d}s' \frac{\delta_1^1(s')}{s'(s'-s)}\right\}$$

is the Omnès function

Omnès, 1958

$\gamma^* \to 3\pi$ dispersive representation

A once-subtracted dispersive solution to the discontinuity equation:

Hoferichter et al., 2014

$$\mathcal{F}(s,q^2) = a(q^2)\Omega(s)\left\{1 + \frac{s}{\pi}\int_{4M_\pi^2}^{\infty} \mathrm{d}s' \frac{\hat{\mathcal{F}}(s',q^2)\sin\delta_1^1(s')}{s'(s'-s)|\Omega(s')|}\right\}$$

$$\Omega(s) = \exp\left\{\frac{s}{\pi}\int_{4M_\pi^2}^{\infty} \mathrm{d}s' \frac{\delta_1^1(s')}{s'(s'-s)}\right\}$$

is the Omnès function

Omnès, 1958

$\hat{\mathcal{F}}(s,q^2)$ absent:

$\mathcal{F}(s,q^2) =$ 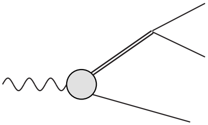

$\hat{\mathcal{F}}(s,q^2)$ present:

$\mathcal{F}(s,q^2) =$ 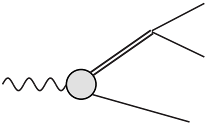 $+$ 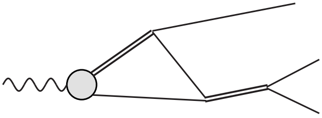 $+\cdots$

- Incorporated crossed-channel interactions

$\gamma^* \to 3\pi$ dispersive representation

$a(q^2)$ fit to different $e^+e^- \to 3\pi$ cross-section data with parameterization:

$$a(q^2) = \frac{F_{3\pi}}{3} + \frac{q^2}{\pi}\int_{s_{\rm thr}}^{\infty} \mathrm{d}s' \frac{\mathrm{Im}\,\mathcal{A}(s')}{s'(s'-q^2)} + C_n(q^2)$$

$$\mathcal{A}(q^2) = \sum_V \frac{c_V}{M_V^2 - q^2 - i\sqrt{q^2}\,\Gamma_V(q^2)}, \qquad V = \omega, \phi, \omega', \omega''$$

$$C_n(q^2) = \sum_{i=1}^{n} c_i\big(z(q^2)^i - z(0)^i\big), \qquad z(q^2) = \frac{\sqrt{s_{\rm inel} - s_1} - \sqrt{s_{\rm inel} - q^2}}{\sqrt{s_{\rm inel} - s_1} + \sqrt{s_{\rm inel} - q^2}}$$

$\gamma^* \to 3\pi$ dispersive representation

$a(q^2)$ fit to different $e^+e^- \to 3\pi$ cross-section data with parameterization:

$$a(q^2) = \frac{F_{3\pi}}{3} + \frac{q^2}{\pi}\int_{s_{\rm thr}}^{\infty} \mathrm{d}s' \frac{\mathrm{Im}\,\mathcal{A}(s')}{s'(s'-q^2)} + C_n(q^2)$$

$$\mathcal{A}(q^2) = \sum_V \frac{c_V}{M_V^2 - q^2 - i\sqrt{q^2}\,\Gamma_V(q^2)}, \qquad V = \omega, \phi, \omega', \omega''$$

$$C_n(q^2) = \sum_{i=1}^{n} c_i \big(z(q^2)^i - z(0)^i\big), \qquad z(q^2) = \frac{\sqrt{s_{\rm inel} - s_1} - \sqrt{s_{\rm inel} - q^2}}{\sqrt{s_{\rm inel} - s_1} + \sqrt{s_{\rm inel} - q^2}}$$

- S-wave cusp eliminated
- Exact implementation of $\gamma^* \to 3\pi$ anomaly:

$$\frac{F_{3\pi}}{3} = \frac{1}{\pi}\int_{s_{\rm thr}}^{\infty} \mathrm{d}s' \frac{\mathrm{Im}\,a(s')}{s'}$$

$e^+e^- \to 3\pi$ cross section data sets

Experiment	Region of $\sqrt{s}\,\mathrm{GeV}$	# data points	Normalization uncertainty
SND 2002	$[0.98, 1.38]$	67	5.0% or 5.4%
SND 2003	$[0.66, 0.97]$	49	3.4% or 4.5%
SND 2015	$[1.05, 1.80]$	31	3.7%
CMD-2 1995	$[0.99, 1.03]$	16	4.6%
CMD-2 1998	$[0.99, 1.03]$	13	2.3%
CMD-2 2004	$[0.76, 0.81]$	13	1.3%
CMD-2 2006	$[0.98, 1.06]$	54	2.5%
DM1 1980	$[0.75, 1.10]$	26	3.2%
ND 1991	$[0.81, 1.39]$	28	10% or 20%
DM2 1992	$[1.34, 1.80]$	10	8.7%
BaBar 2004	$[1.06, 1.80]$	30	all systematics

- Normalization-type systematic uncertainties are assumed to be 100% correlated
- Normalization uncertainties produce a biased fit for an empirical full covariance-matrix minimization

D'Agostini bias & unbiased fits

Simple example of overall normalization uncertainty inducing a bias:

D'Agostini, 1994

$y_1 = 8.0 \pm 2\%$ & $y_2 = 8.5 \pm 2\%$, normalization error of $\epsilon = 10\%$

- Covariance matrix
$$V = \begin{pmatrix} \sigma_1^2 & 0 \\ 0 & \sigma_2^2 \end{pmatrix} + \varepsilon^2 \begin{pmatrix} y_1^2 & y_1 y_2 \\ y_1 y_2 & y_2^2 \end{pmatrix} = \begin{pmatrix} \sigma_1^2 + \varepsilon^2 y_1^2 & \varepsilon^2 y_1 y_2 \\ \varepsilon^2 y_1 y_2 & \sigma_2^2 + \varepsilon^2 y_2^2 \end{pmatrix}$$

- $\chi^2 = \Delta^{\mathrm{T}} V^{-1} \Delta$, $\Delta = \begin{pmatrix} y_1 - \hat{y} \\ y_2 - \hat{y} \end{pmatrix}$

- $\Rightarrow \hat{y} = 7.87 \pm 0.81 < y_1 \,\&\, y_2$ **?**

D'Agostini bias & unbiased fits

- Happens when the data values are rescaled independently of their errors
- Smaller data points are assigned a smaller uncertainty than larger ones

A better covariance matrix:

$$\mathrm{V} = \begin{pmatrix} \sigma_1^2 & 0 \\ 0 & \sigma_2^2 \end{pmatrix} + \varepsilon^2 \begin{pmatrix} \hat{y}^2 & \hat{y}^2 \\ \hat{y}^2 & \hat{y}^2 \end{pmatrix} = \begin{pmatrix} \sigma_1^2 + \varepsilon^2\hat{y}^2 & \varepsilon^2\hat{y}^2 \\ \varepsilon^2\hat{y}^2 & \sigma_2^2 + \varepsilon^2\hat{y}^2 \end{pmatrix}$$

General iterative solution: NNPDF collaboration, 2010

$$\mathrm{V}_{n+1}(i,j) = \mathrm{V}^{\mathsf{stat}}(i,j) + \frac{\mathrm{V}^{\mathsf{syst}}(i,j)}{y_i y_j} f_n(x_i) f_n(x_j)$$

Fit results

- Resonance parameters $M_\omega, \Gamma_\omega, M_\phi, \Gamma_\phi, c_\omega$, c_ϕ, $c_{\omega'}$ & $c_{\omega''}$
- Conformal parameters c_1, c_2 & c_3
- Energy rescaling $\sqrt{s} \to \sqrt{s} + \xi(\sqrt{s} - 3M_\pi)$

	This work
χ^2/dof	430.8/305=1.41

- Fit errors are inflated by the scale factor $S = \sqrt{\chi^2/\text{dof}}$

Fit results

Fit to $e^+e^- \to 3\pi$ data up to $1.8\,\text{GeV}$:

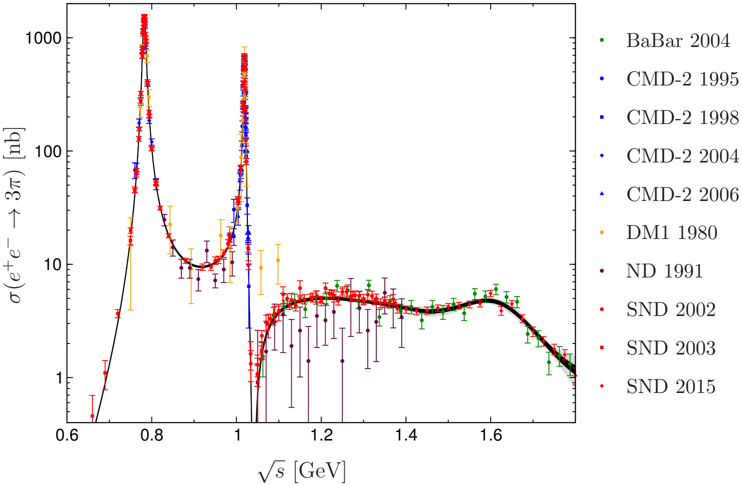

- VP removed from the cross section
- Black and Gray bands represent fit and total uncertainties

Fit results

Enlarged ω and ϕ regions:

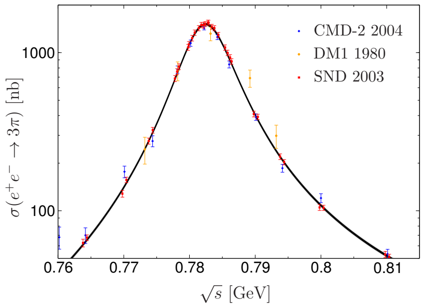

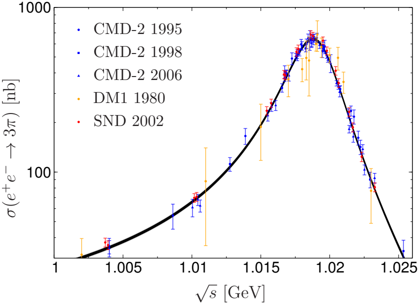

$M_\omega = 782.63(3)\,\text{MeV}$, $\Gamma_\omega = 8.71(6)\,\text{MeV}$

$M_\phi = 1019.20(2)\,\text{MeV}$, $\Gamma_\phi = 4.23(4)\,\text{MeV}$

Compared to PDG (VP-subtraction $\Delta M_\omega = -0.13\,\text{MeV}$, $\Delta M_\phi = -0.26\,\text{MeV}$):

$M_\omega = 782.65(12)\,\text{MeV}$, $\Gamma_\omega = 8.49(8)\,\text{MeV}$

$M_\phi = 1019.461(16)\,\text{MeV}$, $\Gamma_\phi = 4.249(13)\,\text{MeV}$

- M_ω consistent with PDG; tension with $\pi\pi$ persists!

Fit results

Central result for the 3π contribution to HVP:

$$\boxed{a_\mu^{3\pi}|_{\leq 1.8\,\mathrm{GeV}} = 46.2(6)(6) \times 10^{-10} = 46.2(8) \times 10^{-10}}$$

- Interpolation errors $\Rightarrow$ main discrepancy between different groups

Threshold region $a_\mu^{3\pi}|_{\leq 0.66\,\mathrm{MeV}} = 0.02 \times 10^{-10}$

- Twice the estimate from WZW action+vector meson dominance model

Kuraev and Silagadze, 1995, Ahmedov et al., 2002

Fit results

Update after the current analysis:

$a_\mu^{3\pi} \times 10^{10}$ below $1.8\,\mathrm{GeV}$ in WP 2020		
Davier et al., 2019	Keshavarzi et al., 2019	Hoferichter et al., 2019
46.21 ± 1.45	46.63 ± 0.94	46.16 ± 0.82

- Large relative difference resolved

In combination with the 2π channel: Colangelo et al., 2018

$$\boxed{a_\mu^{2\pi}|_{\leq 1.0\,\mathrm{GeV}} + a_\mu^{3\pi}|_{\leq 1.8\,\mathrm{GeV}} = 541.2(2.7) \times 10^{-10}}$$

- 80% of HVP imposing analyticity and unitarity constraints

Hadronic light-by-light scattering

- Previous estimates based on hadronic models except for lattice
- New model-independent initiatives: employ DR to relate dominant contributions to observables like form factors

Colangelo et al., 2014,
Pauk, Vanderhaeghen, 2014

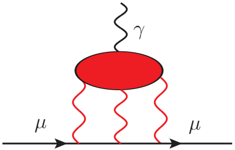

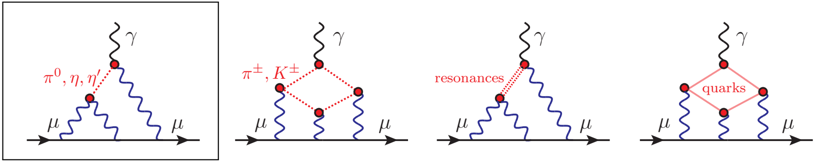

- π^0-pole term is the largest individual contribution to HLbL

Hadronic light-by-light scattering

Comparison between dispersive approach and lattice:

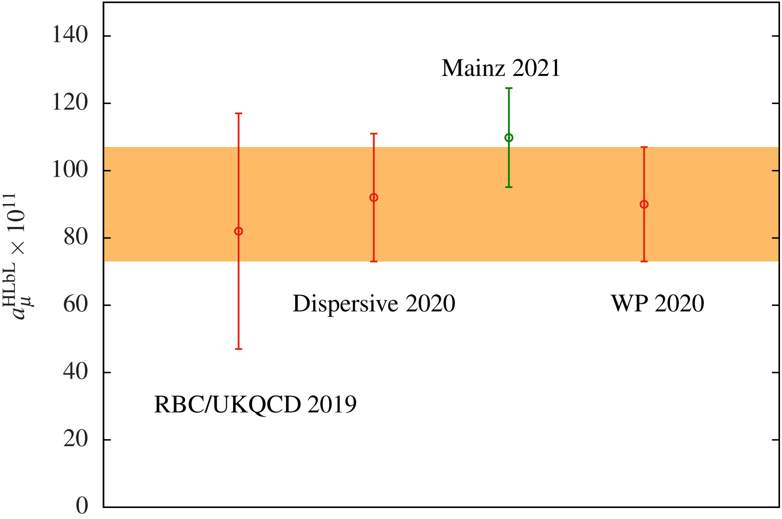

Hadronic light-by-light scattering

A general master formula for the complete HLbL contributions:

Colangelo et al., 2015

$$a_\mu^{\mathrm{HLbL}} = \frac{2\alpha^3}{3\pi^2} \int_0^\infty \mathrm{d}Q_1 \int_0^\infty \mathrm{d}Q_2 \int_{-1}^1 \mathrm{d}\tau \sqrt{1-\tau^2} Q_1^3 Q_2^3 \sum_{i=1}^{12} T_i(Q_1, Q_2, \tau) \bar{\Pi}_i(Q_1, Q_2, \tau)$$

- $T_i(Q_1, Q_2, \tau)$: kernel functions
- $\bar{\Pi}_i(Q_1, Q_2, \tau)$: hadronic scalar functions

The pion pole easily identified with the hadronic functions $\bar{\Pi}_i$:

$$\bar{\Pi}_1^{\pi^0\text{-pole}}(Q_1, Q_2, \tau) = -\frac{F_{\pi^0\gamma^*\gamma^*}(-Q_1^2, -Q_2^2) F_{\pi^0\gamma^*\gamma^*}\big(-(Q_1+Q_2)^2, 0\big)}{(Q_1+Q_2)^2 + M_{\pi^0}^2}$$

$$\bar{\Pi}_2^{\pi^0\text{-pole}}(Q_1, Q_2, \tau) = -\frac{F_{\pi^0\gamma^*\gamma^*}\big(-Q_1^2, -(Q_1+Q_2)^2\big) F_{\pi^0\gamma^*\gamma^*}(-Q_2^2, 0)}{Q_2^2 + M_{\pi^0}^2}$$

Pion-pole contribution—definition

A 3 dimensional representation for the pion-pole contribution:

Knecht, Nyffeler, 2002
Jegerlehner, Nyffeler, 2009

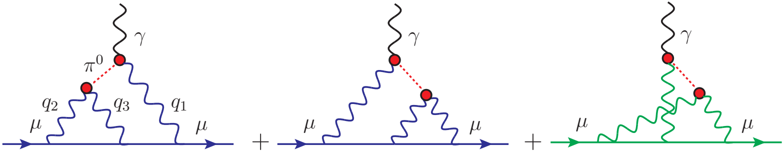

$$a_\mu^{\pi^0\text{-pole}} = \left(\frac{\alpha}{\pi}\right)^3 \int_0^\infty \mathrm{d}Q_1 \int_0^\infty \mathrm{d}Q_2 \int_{-1}^1 \mathrm{d}\tau$$
$$\times \Big[w_1(Q_1, Q_2, \tau)\, F_{\pi^0\gamma^*\gamma^*}(-Q_1^2, -(Q_1+Q_2)^2)\, F_{\pi^0\gamma^*\gamma^*}(-Q_2^2, 0)$$
$$+ w_2(Q_1, Q_2, \tau)\, F_{\pi^0\gamma^*\gamma^*}(-Q_1^2, -Q_2^2)\, F_{\pi^0\gamma^*\gamma^*}(-(Q_1+Q_2)^2, 0) \Big]$$

- $w_1(Q_1, Q_2, \tau)$ & $w_2(Q_1, Q_2, \tau)$: weight functions; concentrated in $Q_i \leq 0.5$ GeV
- $F_{\pi^0\gamma^*\gamma^*}(-Q_1^2, -Q_2^2)$: on-shell space-like pion transition form factors

Pion transition form factor

- Defined by the matrix element of two electromagnetic currents $j_\mu(x)$

$$i\int \mathrm{d}^4x\, e^{iq_1\cdot x}\,\langle 0|T\{j_\mu(x)j_\nu(0)\}|\pi^0(q_1+q_2)\rangle$$
$$= -\epsilon_{\mu\nu\rho\sigma}\, q_1^\rho q_2^\sigma F_{\pi^0\gamma^*\gamma^*}(q_1^2,q_2^2)$$

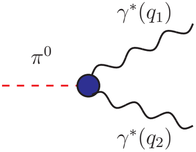

- Normalization fixed by the Adler–Bell–Jackiw anomaly:

$$F_{\pi^0\gamma^*\gamma^*}(0,0) = \frac{1}{4\pi^2 F_\pi} \equiv F_{\pi\gamma\gamma}$$

Pion transition form factor

- Defined by the matrix element of two electromagnetic currents $j_\mu(x)$

$$i\int \mathrm{d}^4x\, e^{iq_1\cdot x}\, \langle 0 | T\{j_\mu(x) j_\nu(0)\} | \pi^0(q_1+q_2)\rangle$$
$$= -\epsilon_{\mu\nu\rho\sigma}\, q_1^\rho q_2^\sigma F_{\pi^0\gamma^*\gamma^*}(q_1^2, q_2^2)$$

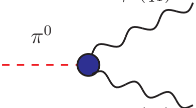

- Normalization fixed by the Adler–Bell–Jackiw anomaly:

$$F_{\pi^0\gamma^*\gamma^*}(0,0) = \frac{1}{4\pi^2 F_\pi} \equiv F_{\pi\gamma\gamma}$$

We build the form factor representation:

$$F_{\pi^0\gamma^*\gamma^*}(q_1^2, q_2^2) = F^{\text{disp}}_{\pi^0\gamma^*\gamma^*}(q_1^2, q_2^2) + F^{\text{eff}}_{\pi^0\gamma^*\gamma^*}(q_1^2, q_2^2) + F^{\text{asym}}_{\pi^0\gamma^*\gamma^*}(q_1^2, q_2^2)$$

- Reconstructed from all lowest-lying singularities
- Fulfills the asymptotic constraints at $\mathcal{O}(1/Q^2)$
- Suitable for a_μ loop-integral evaluation

Pion transition form factor

Dispersive reconstruction from the lowest-lying hadronic intermediate states:

$$F_{\pi^0\gamma^*\gamma^*}(q_1^2, q_2^2) = F_{vs}(q_1^2, q_2^2) + F_{vs}(q_2^2, q_1^2)$$

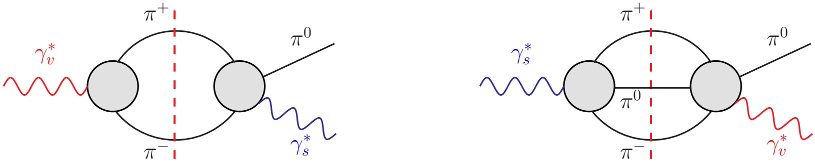

Pion transition form factor

Dispersive reconstruction from the lowest-lying hadronic intermediate states:

$$F_{\pi^0\gamma^*\gamma^*}(q_1^2, q_2^2) = F_{vs}(q_1^2, q_2^2) + F_{vs}(q_2^2, q_1^2)$$

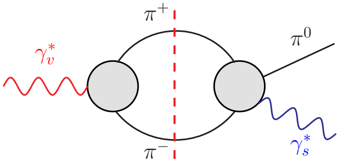

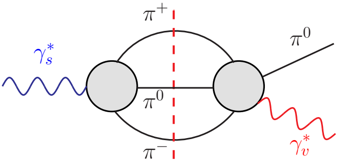

Isovector photon: 2 pions

- $\gamma_v^* \to \pi^+\pi^- \to \gamma_s^*\pi^0$
- $\mathrm{disc} \propto$ pion vector form factor $\times$ $\gamma_s^* \to 3\pi$ amplitude

Isoscalar photon: 3 pions

- $\gamma_s^* \to \pi^+\pi^-\pi^0 \to \gamma_v^*\pi^0$
- Dominated by resonances ω, ϕ, ω', & ω''

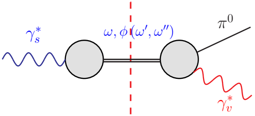

Pion transition form factor

Dispersive reconstruction from the lowest-lying hadronic intermediate states:

$$F_{\pi^0\gamma^*\gamma^*}(q_1^2, q_2^2) = F_{vs}(q_1^2, q_2^2) + F_{vs}(q_2^2, q_1^2)$$

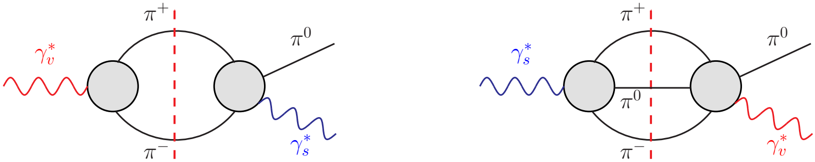

Building blocks of the dispersive treatment:

- Pion vector form factor $F_\pi^V(s)$
- Partial wave amplitude $f_1(s, q^2)$ for the $\gamma_s^*(q) \to \pi^+\pi^-\pi^0$ reaction

Pion transition form factor

Fit $a(q^2)$ to different $e^+e^- \to 3\pi$ cross-section data with:

- S-wave cusp eliminated
- Exact implementation of $\gamma_s^*(q) \to 3\pi$ anomaly

$$\frac{F_{3\pi}}{3} = \frac{1}{\pi}\int_{s_{\text{thr}}}^{\infty} \mathrm{d}s' \frac{\operatorname{Im} a(s')}{s'}$$

- Asymptotic behavior of $C_n(q^2)$ controlled

Pion transition form factor

6 (7) parameters c_ω, c_ϕ, $c_{\omega'}$, $c_{\omega''}$, c_1, c_2 & (c_3) fit to $e^+e^- \to 3\pi$ data:

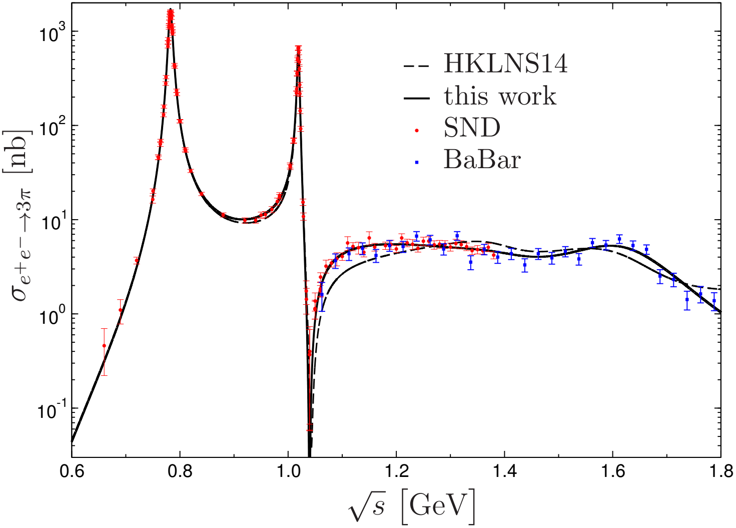

- Substantially improved above the ϕ peak

Pion transition form factor

Double-spectral representation of the form factor:

$$F^{\mathsf{disp}}_{\pi^0\gamma^*\gamma^*}(-Q_1^2,-Q_2^2) = \frac{1}{\pi^2}\int_{4M_\pi^2}^{s_{\mathsf{iv}}} \mathsf{d}x \int_{s_{\mathsf{thr}}}^{s_{\mathsf{is}}} \frac{\rho^{\mathsf{disp}}(x,y)\,\mathsf{d}y}{\left(x+Q_1^2\right)\left(y+Q_2^2\right)},$$

$$\rho^{\mathsf{disp}}(x,y) = \frac{q_\pi^3(x)}{12\pi\sqrt{x}}\mathsf{Im}\left[\left(F_\pi^V(x)\right)^* f_1(x,y)\right] + [x \leftrightarrow y]$$

$f_1(s,q^2) = \mathcal{F}(s,q^2) + \hat{\mathcal{F}}(s,q^2)$: $\gamma_s^*(q) \to 3\pi$ P-wave

Pion transition form factor

Effective pole term:

$F^{\text{disp}}_{\pi^0\gamma^*\gamma^*}(q_1^2, q_2^2)$ fulfills the chiral anomaly $F_{\pi\gamma\gamma}$ by around 90%

$\Rightarrow$ Introduce an effective pole term

$$F^{\text{eff}}_{\pi^0\gamma^*\gamma^*}(q_1^2, q_2^2) = \frac{g_{\text{eff}}}{4\pi^2 F_\pi} \frac{M_{\text{eff}}^4}{(M_{\text{eff}}^2 - q_1^2)(M_{\text{eff}}^2 - q_2^2)}$$

g_{eff} fixed by fulfilling the chiral anomaly

$g_{\text{eff}} \sim 10\%$, $\Rightarrow$ small

M_{eff} fit to singly-virtual data excluding BaBar above $5\,\text{GeV}^2$ Gronberg et al., 1998, Aubert et al., 2009, Uehara et al., 2012

$M_{\text{eff}} \sim 1.5$–$2\,\text{GeV}$, $\Rightarrow$ reasonable

Pion transition form factor

Asymptotically, $F_{\pi^0\gamma^*\gamma^*}$ should fulfill Brodsky, Lepage, 1979-1981

$$F_{\pi^0\gamma^*\gamma^*}(q_1^2, q_2^2) = -\frac{2F_\pi}{3}\int_0^1 \mathrm{d}x \frac{\phi_\pi(x)}{xq_1^2 + (1-x)q_2^2} + \mathcal{O}\left(\frac{1}{q_i^4}\right),$$

Pion distribution amplitude $\phi_\pi(x) = 6x(1-x) + \cdots$

Brodsky–Lepage (BL) limit:

$$\lim_{Q^2\to\infty} F_{\pi^0\gamma^*\gamma}(-Q^2, 0) = \frac{2\,F_\pi}{Q^2}$$

Operator product expansion (OPE): Nesterenko, Radyushkin, 1983, Novikov et al., 1984, Manohar, 1990

$$\lim_{Q^2\to\infty} F_{\pi^0\gamma^*\gamma^*}(-Q^2, -Q^2) = \frac{2\,F_\pi}{3\,Q^2}$$

Pion transition form factor

Rewrite the asymptotic form into a double-spectral representation:

$$F^{\text{asym}}_{\pi^0\gamma^*\gamma^*}(q_1^2, q_2^2) = \frac{1}{\pi^2}\int_0^\infty \int_0^\infty \mathrm{d}x\mathrm{d}y \frac{\rho^{\text{asym}}(x,y)}{(x-q_1^2)(y-q_2^2)},$$

$$\rho^{\text{asym}}(x,y) = -2\pi^2 F_\pi xy\delta''(x-y)$$

Decomposition of the pion-transition form factor:

$$F_{\pi^0\gamma^*\gamma^*}(q_1^2, q_2^2) = \frac{1}{\pi^2}\int_0^{s_\text{m}} \mathrm{d}x \int_0^{s_\text{m}} \mathrm{d}y \frac{\rho^{\text{disp}}(x,y)}{(x-q_1^2)(y-q_2^2)} + \frac{1}{\pi^2}\int_{s_\text{m}}^\infty \mathrm{d}x \int_{s_\text{m}}^\infty \mathrm{d}y \frac{\rho^{\text{asym}}(x,y)}{(x-q_1^2)(y-q_2^2)}$$
$$+ \frac{1}{\pi^2}\int_0^{s_\text{m}} \mathrm{d}x \int_{s_\text{m}}^\infty \mathrm{d}y \frac{\rho(x,y)}{(x-q_1^2)(y-q_2^2)} + \frac{1}{\pi^2}\int_{s_\text{m}}^\infty \mathrm{d}x \int_0^{s_\text{m}} \mathrm{d}y \frac{\rho(x,y)}{(x-q_1^2)(y-q_2^2)}$$

- s_m: continuum threshold
- $\rho(x,y)$ not known rigorously, $\rho^{\text{asym}}(x,y)$ applied in mixed regions vanishes

  $\Rightarrow$ All constraints can be fulfilled discarding mixed regions

Pion transition form factor

This defines the asymptotic contribution:

$$F^{\mathsf{asym}}_{\pi^0\gamma^*\gamma^*}(q_1^2, q_2^2) = 2F_\pi \int_{s_\mathrm{m}}^{\infty} \mathsf{d}x \frac{q_1^2 q_2^2}{(x - q_1^2)^2 (x - q_2^2)^2}$$

- Does not contribute for the singly-virtual kinematics
- Restores the asympotics for singly-/doubly-virtual kinematics

The final representation:

$$F_{\pi^0\gamma^*\gamma^*}(q_1^2, q_2^2) = F^{\mathsf{disp}}_{\pi^0\gamma^*\gamma^*}(q_1^2, q_2^2) + F^{\mathsf{eff}}_{\pi^0\gamma^*\gamma^*}(q_1^2, q_2^2) + F^{\mathsf{asym}}_{\pi^0\gamma^*\gamma^*}(q_1^2, q_2^2)$$

Numerical results

Uncertainty estimates:

- The uncertainty in $F_{\pi\gamma\gamma}$ at 0.8% from PrimEx II — Larin et al., 2020
  - Varying the coupling g_{eff}
- Dispersive uncertainties estimated by
  - Varying the cutoffs between 1.8 and $2.5\,\mathrm{GeV}$
  - Different $\pi\pi$ phase shifts — Caprini et al., 2012, García-Martín et al., 2011, Schneider et al., 2012
  - Different representations of $F_\pi^V(s)$
  - Different conformal polynomial fits to $e^+e^- \to 3\pi$

Numerical results

Uncertainty estimates:

- The uncertainty in $F_{\pi\gamma\gamma}$ at 0.8% from PrimEx II — Larin et al., 2020
  - Varying the coupling g_{eff}
- Dispersive uncertainties estimated by
  - Varying the cutoffs between 1.8 and $2.5\,\text{GeV}$
  - Different $\pi\pi$ phase shifts — Caprini et al., 2012, García-Martín et al., 2011, Schneider et al., 2012
  - Different representations of $F_\pi^V(s)$
  - Different conformal polynomial fits to $e^+e^- \to 3\pi$
- BL limit uncertainty by $^{+20}_{-10}\%$ — Aubert et al., 2009, Uehara et al., 2012
  - Varying the mass parameter M_{eff}
  - Completely covers 3σ band
- Asymptotic part $s_{\text{m}} = 1.7(3)\,\text{GeV}^2$ — Khodjamirian, 1999, Agaev et al., 2011, Mikhailov et al., 2016
  - Expected from light-cone sum rules

Numerical results

Singly-virtual space-like transition form factor in $Q^2 F_{\pi^0\gamma^*\gamma^*}(-Q^2, 0)$:

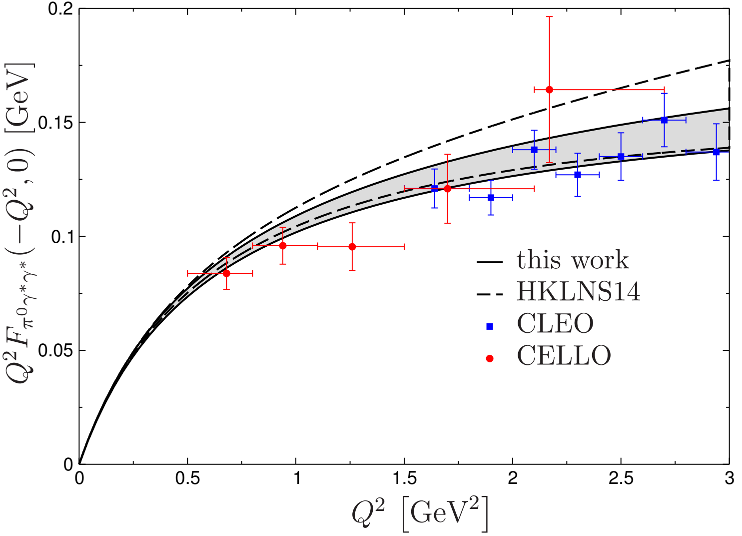

Numerical results

Singly-virtual space-like transition form factor in $Q^2 F_{\pi^0\gamma^*\gamma^*}(-Q^2, 0)$:

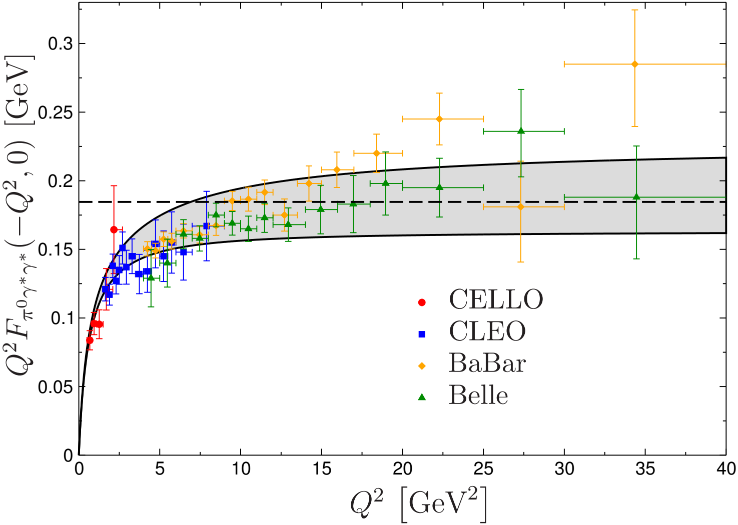

Numerical results

Diagonal form factor in $Q^2 F_{\pi^0\gamma^*\gamma^*}(-Q^2, -Q^2)$ in comparison to lattice:

Gérardin et al., 2019

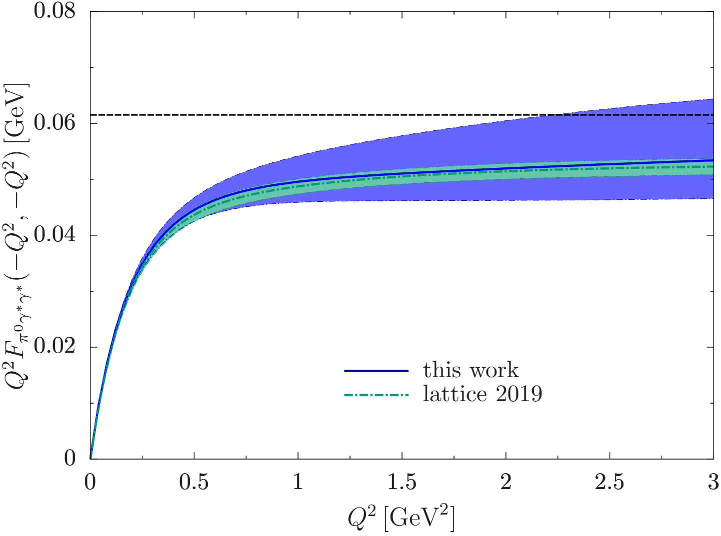

Numerical results

Diagonal form factor in $Q^2 F_{\pi^0\gamma^*\gamma^*}(-Q^2,-Q^2)$ in comparison to LMD+V fit to lattice: Gérardin et al., 2016

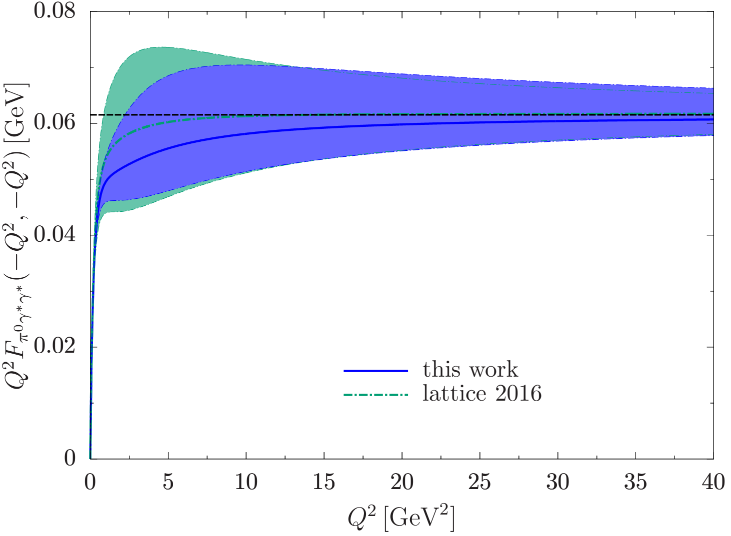

Numerical results

$(Q_1^2 + Q_2^2) F_{\pi^0\gamma^*\gamma^*}(-Q_1^2, -Q_2^2)$ as a function of Q_1^2 and Q_2^2:

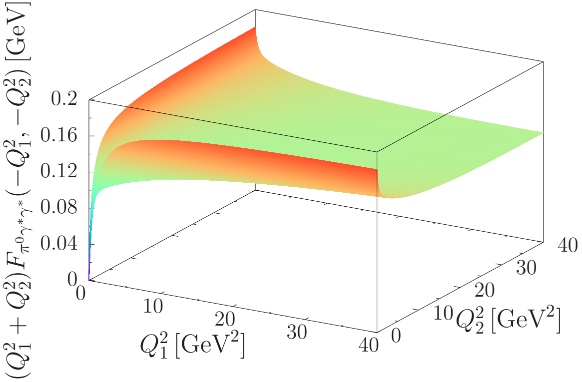

- $1/Q_i^2$ behavior in the entire domain of space-like virtualities

  $\Rightarrow$ Hard to obtain in resonance models

Numerical results

Pion-pole contribution to a_μ from the final representation:

$$\begin{aligned} a_\mu^{\pi^0\text{-pole}} &= 63.0(0.9)_{F_{\pi\gamma\gamma}}(1.1)_{\text{disp}}\binom{2.2}{1.4}_{\text{BL}}(0.6)_{\text{asym}} \times 10^{-11} \\ &= 63.0^{+2.7}_{-2.1} \times 10^{-11} \end{aligned}$$

- First complete data-driven determination
- Fully controlled uncertainty estimates

Comparison to lattice:

- Lattice 2016: $(65.0 \pm 8.3) \times 10^{-11}$ Gérardin et al., 2016
- Lattice 2019: $(59.7 \pm 3.6) \times 10^{-11}$, changes to $(62.3 \pm 2.3) \times 10^{-11}$ after fixing normalization from experiment Gérardin et al., 2019

Conclusion and outlook

- Hadronic vacuum polarization: 3π
  - Independent dispersive analysis for the 3π channel
  - Resolved main tension in 3π, reaffirmed tension in a_μ
- Hadronic light-by-light scattering: pion pole
  - Dispersive reconstruction of the pion transition form factor
  - Data-driven determination of $a_\mu^{\pi^0\text{-pole}}$ with carefully estimated improvable uncertainties
- Similar analysis done for $\pi^0\gamma$ — Hoid et al. 2020
- $\pi^0 \to e^+e^-$ — Hoferichter et al. 2021
- η and η' pole contributions — S. Holz et al.


Much obliged for your attention!